Spatial Variation in Demographic Processes and the Potential Role of Hybridization to Future Persistence

Meaghan R Gade (meaghan.gade@yale.edu)
The Ohio State University https://orcid.org/0000-0001-7309-5934
Qing Zhao
University of Missouri
William E Peterman
The Ohio State University

Research Article

Keywords: demography, true survival, spatially explicit integrated population model, life history, Plethodon, hybrid, climate change

Posted Date: September 24th, 2021

DOI: https://doi.org/10.21203/rs.3.rs-832663/v1

Spatial variation in demographic processes and the potential role of hybridization to future persistence

Meaghan R. Gade[1,3], Qing Zhao[2], and William E. Peterman[1]

[1]School of Environment and Natural Resources, The Ohio State University, Columbus OH 43201

[2] School of Natural Resources, University of Missouri, Columbia MO, USA

[3] Corresponding Author: Present address: Department of Ecology and Evolutionary Biology, Yale University, New Haven, CT; email: meaghan.gade@yale.edu

Abstract

CONTEXT

Spatial variation in life history traits plays a crucial role in the structure and dynamics of populations. The demographic responses of local populations to fine-scale habitat heterogeneity have consequences for species at a broader scale and responses vary across spatial scales. Yet, the specific nature of such relationships is unclear across taxa.

OBJECTIVES

We evaluated the spatial variation in demographic traits of cryptic terrestrial salamanders across the broad scale environmental gradient of elevation (i.e. temperature) and the fine-scale gradient of stream distance (i.e. moisture).

METHODS

Using a 4-years of spatial mark-recapture and count data, we implemented a spatially explicit Integrated Population Model to understand demographic rates across scales. We also investigated how hybridization, which occurs in between lungless salamanders at mid-elevations, may influence demographic rates.

RESULTS

We found that high elevation animals grow faster and move more, especially far from streams likely as a result of increased temperatures. Survival was highest but recruitment rates were lowest at low elevations and significantly declined with distance to stream. We also found that hybrid animals at low elevations had higher survival probabilities.

CONCLUSIONS

Our study reveals nuanced spatial variation in demographic rates that differ in magnitude depending on the scale at which they are assessed. Our results also show animals

exhibit demographic compensation across abiotic gradients, underscoring the need for further conservation and management efforts to implement spatially explicit and dynamic strategies to match the demographic variation of species and populations of species separated across space.

Keywords: demography; true survival; spatially explicit integrated population model; life history; Plethodon; hybrid; climate change

Introduction

Landscapes are inherently heterogeneous in both biotic and abiotic features across spatial scales and life history traits are expected to covary in response to such heterogeneity (Wiens et al. 1993). Microhabitats are a strong driver of life history variation because environmental conditions experienced by individuals at a fine scale can be very different from conditions measured at a broader scale. For example, the breeding success of red billed choughs (*Pyrrhocorax pyrrhocorax)* differs between individual nest sites but not across a larger spatial scale, suggesting local-scale variation in habitat likely drives this demographic parameter (Reid et al. 2006; Sullivan and Vierling 2012). The role of microhabitats are particularly salient for small-bodied organisms like amphibians or small mammals, for example, which interact with the landscape at a fine-scale and experience an environment buffered from broader landscape conditions (Riddell et al. 2021). Understanding fine-scale spatial heterogeneity of demographic rates will provide a clearer understanding of species dynamics across a broader landscape and inform species monitoring and management efforts.

The growing threats from climate change hasten the need for local-scale demographic data. Climate change can have differential impacts on species throughout their range depending on habitat, resources, species adaptive capacity, among others (Urban et al. 2016). These effects may be particularly pronounced for organisms that are highly sensitive to habitat disturbances and have limited dispersal capacity, such as many amphibian species. In response to climate change, organisms may modify their behavior, physiology preferences, and/or alter their geographic ranges to track their optimal climate niche (MacLean and Beissinger 2017). In montane regions, upward range shifts may be limited for high elevation species due to already constrained geographic ranges and ever-decreasing habitat availability at the highest elevation (Elsen and Tingley 2015). For such high-elevation isolates, or “sky island” species,

63 counteracting mortality from extreme conditions with recruitment and/or immigration from other
64 populations is limited, increasing the threat to high elevation population declines (Brown and
65 Kodric-Brown 1977). As a consequence of upward range shifts in montane habitats, some
66 species have modified (e.g., Taylor et al. 2014) and/or formed novel (e.g., Garroway et al. 2010)
67 hybrid zones. Hybridization can provide a unique solution to climate change by providing
68 genetic variation that may facilitate local adaptation within a single to few generations
69 (Seehausen 2004). In fact, there are reports of hybrid taxa outperforming parental species,
70 especially in extreme, marginal, or novel environments (Willis et al. 2006; Chunco et al. 2012).
71 For organisms that lack evolutionary capacity to keep pace with climate change due to long
72 generation times, low gene flow, or narrow physiological tolerances (Ficke et al. 2007),
73 hybridization could be an important mechanism to allow population persistence in the future
74 (Chunco 2014).

75 Amphibians are among the most endangered vertebrate taxa as a result of not only
76 climate change, but also disease, habitat loss, and invasive species (Blaustein et al. 2011; Grant
77 et al. 2016). Despite their clear importance to contributing to myriad ecosystem services
78 including nutrient cycling, biological control, bioturbation, and decomposition (Valencia-Aguilar
79 et al. 2013; Hocking and Babbitt 2014), we have little understanding of basic demographic rates
80 for most amphibian species. Without such data, we are severely limited in our ability to
81 effectively conserve and predict species persistence in the future. Amphibians in the family
82 Plethodontidae are particularly susceptible to the effects of climate change in part because these
83 salamanders lack lungs and rely on cool and wet conditions to facilitate gas exchange across the
84 skin surface. As such, any disruptions to their microclimate and habitat may be potentially
85 catastrophic to survival (Feder and Londos 1984). In the Southern Appalachian Mountains,

where the highest abundance and species richness of terrestrial *Plethodon* exists, there are multiple hybrid zones between terrestrial *Plethodon* species. One of the most well-studied is that of *P. teyahalee* and *P. shermani* in the Nantahala Mountains of North Carolina (Hairston, Wiley, Smith, & Kneidel, 1992; Walls, 2009). Hairston et al. (1992) showed that the hybrid zone between these two species has moved upward, with the proportion of individuals with traits of *P. teyahalee,* the low elevation species, increasing with elevation over a 16-year period. Walls (2009) attributed this upward shift to increasing temperatures across elevations. To understand the role hybridization may play in the survival of species requires a detailed knowledge of demographic vital rates of both parent and hybrid. Yet for many *Plethodon* salamanders, we know virtually nothing about their fine-scale demographic vital rates, especially as they relate to spatial variation (but see Caruso and Rissler 2018).

Many significant challenges for measuring demographic rates at fine scales exist including time, labor, and cost intensive sampling. A common method for estimating demographic rates is capture-mark-recapture (CMR) whereby individuals within a population are uniquely marked over a period of time and survival and recruitment are subsequently estimated. However, traditional CMR analyses including Cormack-Jolly-Seber (CJS) models cannot distinguish between emigration and mortality, thereby severely biasing apparent survival rates (Marshall et al. 2004; Schaub and Royle 2014). The development of spatially explicit CJS (sCJS) models ameliorate this bias by incorporating specific capture locations to identify when dispersal or emigration has occurred at each plot, allowing for the estimation of true, instead of the traditional apparent survival (Schaub and Royle 2014). However, with this statistical advancement comes the requirement for a large amount of CMR data to obtain reliable estimates. Also, the sCJS model still does not provide a comprehensive understanding of metapopulation

dynamics. Integrated population models (IPM) have been increasingly applied in ecological research as an elegant solution to intensive, long-term data collection as they can estimate latent parameters that have not been measured directly (Schaub and Abadi 2011). IPMs also leverage numerous data sources including CMR, repeated counts, reproduction, among others, to account for multiple sources of uncertainty to more accurately and precisely estimate demographic parameters (Schaub and Abadi 2011). Further, spatially explicit IPMs (SEIPM) allow for heterogeneity in reproduction and survival processes based on the spatial variation in the landscape, density dependent processes, and dispersal between habitat patches (Zhao 2020). SEIPMs also are more flexible in the data inputs and can accommodate large amounts of count data with smaller amounts of CMR data. Count data is typically far simpler to collect in space and time in comparison to the time-consuming and expensive CMR data collection, adding an additional benefit to SEIPM.

In this study, we use three different models to understand spatial patterns in demographic parameters for terrestrial salamanders across a montane landscape to understand how demographic variation at fine scales are constrained by broader scale patterns. The Southern Appalachian Mountains are characterized by stark abiotic gradients that shape the distribution and abundance of terrestrial *Plethodon* across scales. Gade and Peterman (2019) found that at low elevations, where the regional climate is hot and dry, salamanders are distributed and in the highest abundance near stream sides. Stream sides offer a microhabitat that is cooler and moister than the surrounding landscapes. However, at high elevations, salamanders are distributed more uniformly across the landscape and are less tied to stream sides since the regional climate at high elevations is more broadly cool and wet (Gade & Peterman, 2019). The dynamics of broad-scale elevation and local-scale stream distance gradients interact to drive the distribution of these

132 salamanders, yet we do not understand how population dynamics vary across these gradients.
133 Using 4 years of CMR data and 3 years of count data, we attempt to fill this knowledge gap to
134 provide an understanding of both fine-scale and landscape-scale spatial dynamics of terrestrial
135 *Plethodon* salamander population demographics.
136
137 **Methods**
138 *Capture-Mark-Recapture Surveys*
139 We initiated a long-term spatial capture-mark-recapture (sCMR) study in 2017 to assess
140 salamander demographics and life history across elevation and moisture gradients. Twelve plots,
141 10m x 10m in size, gridded off in 1-m^2 sections, were spatially arranged to capture an elevation
142 and moisture gradient on Wayah Mountain, Macon County, North Carolina (35.158, -83.574).
143 Specifically, six plots were situated at low elevation (~900 m) and six plots were at high
144 elevation (~1500 m). At each elevation, two replicate sets of three plots were < 5 m of a stream
145 (close), between ~100 – 150 m from a stream (medium), and >190 m from a stream (far) (Fig. 1).
146 Each plot was centered within a larger 20 m x 20 m plot that was sampled for captured animals
147 only to more precisely estimate movement rates. To minimize extraneous variation, forest stand,
148 slope, aspect, and stream order were standardized to the best extent possible among plots
149 (Supporting Information Table 1).
150 We conducted nocturnal area-constrained surveys of each plot whereby at least two
151 observers exhaustively searched plots and hand captured surface-active salamanders, recording
152 their specific capture location to within 1 m^2. We conducted at least 3 (maximum= 5) surveys
153 each year from 2017–2020 during salamander active season, between May and August. Captured
154 salamanders were placed in a sealable bag with moist leaf litter and transported to Highlands
155 Biological Station, approximately 60 km away. At each plot during each survey, we measured

156 environmental covariates including surface soil temperature, soil temperature at 10 cm below
157 ground, air temperature, and relative humidity using an infrared thermometer (Raytek MT4), soil
158 temperature probe, and Kestrel 5200.

159 Salamanders were housed at Highlands Biological Station in a 10°C environmental
160 chamber to limit their metabolism (Connette, 2014) until processing occurred within 24 hours of
161 each survey. We anesthetized each salamander in an Orajel solution (1g/1L) and uniquely
162 marked them with a visual implant elastomer (Northwest Marine Technologies, LLC). Visual
163 implant elastomer are commonly used to tag amphibians and have minimal effects on survival
164 and are more permananet than other marking techniques (e.g. toe clipping; Bailey 2004,
165 Oropeza–Sánchez et al. 2020). We also recorded morphometric data including snout-vent-length
166 (SVL), sex, and a photograph of the dorsum of each individual using an iPhone 6S+. We then
167 returned salamanders to their capture location (within 1 m) within 48 hours of initial capture.

168 *Hybrid quantification*

169 Our study region was within a known hybridization zone of *P. teyahalee* and *P.shermani,*
170 (Hairston et al., 1992; Highton & Peabody, 2000; Walls, 2009). *Plethodon teyahalee* are
171 distinctly characterized by white spots across their body and *P. shermani* are characterized by
172 red coloration on the legs. Thus, we quantified hybridization from photographs by estimating the
173 percent of each leg covered with red coloration and counting the number of white dots on 4 body
174 regions: (1) head, (2) anterior dorsum, (3) posterior dorsum, and (4) tail (Supporting Information
175 Fig. 1A). We loaded the percent red and spotting scores into a Principal Components Analysis to
176 find a composite measure of 'hybridization'. Dimension 1 accounted for 49.2% of the variation,
177 and we subsequently used the Dimension 1 scores for each individual in the growth and sCJS
178 modeling discussed below. Hybrid scores ranged from -4.28 to 2.20 with negative values

179 indicating more hybrid characteristics and positive values indicating more 'pure' *P. shermani*
180 characteristics (Supporting Information Fig. 1B). While hybrids were only observed at low
181 elevations, there was variation in the hybrid score across elevation due to the variation in leg
182 coloration. Our scoring method accounts only for the observed phenotypic traits of hybrids,
183 neglecting genetic variability or gene combinations, and should thus be considered a coarse
184 metric of hybridization.

185 *Count surveys*

186 We established 87-paired (total plots = 174) count plots, each 3 x 3 m in size situated across
187 elevation (700 – 1550 m) and stream-distance (0 – 250 m) gradients. Each plot was visually
188 surveyed for surface active salamanders between 2130 and 0230 EST. We estimated the age
189 (juvenile or adult) of each counted individual by visual estimation of snout-vent-length (SVL),
190 whereby adults were > 45 mm. Plots were surveyed 4 times in 2017 and once in 2018 and 2019.
191 Specific details of the count data can be found in Gade and Peterman (2019).

192 *Modeling Approaches*

193 *Growth Model*

194 We estimated the effect of elevation, stream distance, preciptitaion, and hybridization score on
195 individual growth during the active season using Fabens formulation of the von Bertalanffy
196 curve growth model (Fabens 1965). We used the average SVL of an individual if it was captured
197 multiple times over a single year and we only included animals captured over at least two years.
198 Since the sCMR plots were arranged at high and low elevation, we included elevation as a binary
199 variable and stream distance as a continuous variable. We calculated the cumulative precipitation
200 for the active season 01 May to 31 August for each survey year from the North Carolina Climate
201 Retrieval and Observation Network of the Southeast Database (https://climate.ncsu.edu/cronos).

202 The growth function was defined for individual *i* at time *t* as:

$$SVL0_{i,t} = SVL0_{i,t-1} + \left\{L - SVL0_{i,t-1} \times \left[1 - exp\left(-K_{i,t} \times \frac{I}{365}\right)\right]\right\} \quad (1)$$

where asymptotic size, L, was estimated as a function of categorical elevation (*ELE*; low, high) as:

$$L = L_0 + L_i \times ELE_i \quad (2)$$

$SVL0_{i,t}$ *i*s size at first capture and follows a Uniform distribution with a minimum of 10 and maximum of 80*,* L_0 was estimated from a Normally distributed prior with a mean of 60 and precision of 0.01 while L_1 was estimated from a Normally distributed prior with a mean of 0 and precision of 0.01. *K* represents the individual growth rate, and *I* is the annual scaling interval between captures. We considered *K* as a function of categorical elevation (high/low), and continuous distance to stream (*STR*), precipitation (*PREC*), and hybrid status (*HYB*) such that:

$$K_{i,t} = \beta_0^{[K]} + \beta_1^{[K]} \times ELE_i + \beta_2^{[K]} \times STR_i + \beta_3^{[K]} \times ELE_i \times STR_i + \beta_4^{[K]} \times PREC_t + \beta_5^{[K]} \times HYB_s + \beta_6^{[K]} \times ELE_i \times HYB_s \quad (3)$$

We used vague normal priors for all growth rate covariates with a mean of 0 and precision of 0.01. We fit the model in JAGS (Plummer 2003) using *jagsUI* (Kellner 2017). Following a burn in of 1,000 and adaptation phase of 5,000, 5 MCMC chains were run for 12,000 iterations, thinned at a rate of 5 for a total posterior sample of 18,220.

We then used the growth rates to estimate time to maturity at both high and low elevations. For high elevations, we estimated time to maturity based on the size of the smallest gravid female *P. shermani* as estimated by Connette (2014), 49.4 mm, because we did not capture any gravid females during our surveys. For low elevations, we estimated the size of

maturity for *P. shermani* hybrids to be 57 mm, based on the nearest reported estimate of size at maturity of a closely related species to *P. teyahalee, P. glutinosis,* in Giles County, VA (Highton 1962). We then averaged the mature sizes of *P. glutinosis* and *P. shermani* (53 mm) because hybrid individuals often exhibit traits intermediate of their parent species (Seehausen 2004). We used the average hatchling size at high elevation (19.15 mm) and low elevation (22.09 mm) as the starting size to generate two growth curves (Connette, 2014).

Spatial Cormack-Jolly-Seber Model

We used a spatial Cormack-Jolly-Seber (sCJS) model (Schaub and Royle 2014) to examine the spatial variation in survival and dispersal. A sCJS model differs from traditional CJS models by incorporating locations of each individual relative to the study area; in our study, spatial locations refer to the 1-m^2 grid cell each salamander was captured. The model assumes that death, birth, immigration, and emigration could occur between, but not within years and equal recapture probability across all individuals and years. The true latent status of an individual *i* at time *t*, $z_{i,t}$ (1 for alive and 0 for dead), was modeled with a Bernoulli distribution given the status in the previous time step and survival probability such that:

$$z_{i,t}|z_{i,t-1} \sim Bernoulli\left(z_{i,t-1} \times \phi_{i,t-1}\right) \qquad (4)$$

in which survival probability ($\phi_{i,t}$) was modeled as a function of categorical elevation (high/low), continuous stream distance, and individual hybrid scores such that:

$$logit\left(\phi_{i,t}\right) = \beta_0^{[\phi]} + \beta_1^{[\phi]} \times ELE_i + \beta_2^{[\phi]} \times STR_i + \beta_3^{[\phi]} \times ELE_i \times STR_i + \beta_4^{[\phi]} \times HYB_i + \beta_5^{[\phi]} \times ELE_i \times HYB_i \qquad (5)$$

247 Survival estimates were scaled to annual survival by including a term indicating the length of
248 time between capture periods.

249 The change in location (G) for individual *i* between the time *t* ($G_{i,t}$) and time *t*+1 ($G_{i,t+1}$) is
250 modeled using a random walk (Turchin and Thoeny 1993) such that:

251 $$G_{i,t+1} \sim Normal\left(G_{i,t}, \chi_i^2\right) \quad (6)$$

252

253 in which the variance χ_i^2 is a function of covariates such that:

254 $$log(\chi_i^2) = \beta_0^{[\chi]} + \beta_1^{[\chi]} \times ELE_i + \beta_2^{[\chi]} \times STR_i + \beta_3^{[\chi]} \times ELE_i \times STR_i + \beta_4^{[\chi]} \times HYB_i + \beta_5^{[\chi]} \times ELE_i \times HYB_s \quad (7)$$

255

256 Thus, the metric of dispersal is a measure of activity center variance between survey periods
257 (Munoz et al. 2016; Schaub and Royle 2014).

258 The observation process of the model which is conditional on survival and presence in
259 the study area, indicated by a step function of whether individual *i* is inside ($r_{i,t} = 1$) or outside
260 ($r_{i,t} = 0$) of the study area at time *t*. The observation process is then expressed as:

261 $$y_{i,t} | z_{i,t}, r_{i,t} \sim Bernoulli\left(z_{i,t} \times r_{i,t} \times p_{i,t}\right) \quad (8)$$

262

263 where $p_{i,t}$ is the recapture probability of individual *i* at time *t*. We modeled recapture probability
264 as a function of air temperature (ATEMP), relative humidity (HUMID), and surface soil
265 temperature (STEMP) such that:

266 $$logit\left(p_{i,t}\right) = \beta_0^{[p]} + \beta_1^{[p]} \times ATEMP_t + \beta_2^{[p]} \times HUMID_t + \beta_3^{[p]} \times STEMP_t \quad (9)$$

267 We used vague normal priors for all covariates with a mean of 0 and precision of 0.01. We fit the
268 model in JAGS (Plummer 2003) using *jagsUI* (Kellner 2017). Following a burn in of 75,000 and

adaptation phase of 60,000, 10 MCMC chains were run for 165,000 iterations, thinned at a rate of 5 for a total posterior sample of 305,000.

Spatially Explicit Integrated Population Model-

We used a spatially explicit integrated population model (SEIPM) to account for spatiotemporal variation in initial population size, immigration, emigration, survival, and per capita reproduction rate in relation to habitat and density covariates (Zhao 2020). This model jointly analyzes count and CMR data by combining a spatially explicit dynamic N-mixture model (Zhao et al. 2017) with a multistate capture-recapture model. The particular benefit of the SEIPM in this study is that it allowed us to leverage multiple data sets that spanned different spatial, temporal, and information coverage for more robust demographic estimation. Unlike the sCJS model, SEIPM allowed for estimations along continuous stream and elevation gradients because of the spatial distribution of the count plots.

For the purposes of the SEIPM, we split the landscape into 100 x 100 m grids and combined the counts of all plots within a grid to reduce the total number of plots from 174 to 50 and reduce overall variation. The model with reduced number of plots resulted in improved mixing of MCMC chains and more efficient sampling of posterior distributions, in comparison to the same model with the original number of plots. Six of the twelve capture-recapture plots overlapped spatial locations with count plots (Fig. 1). We did not include hybrid score in this analysis because we did not photograph salamanders from the count plots.

The SEIPM model is a hierarchical Bayesian model containing a process model which describes how local population sizes vary spatially and temporally and an observation model which describes how count and CMR data are obtained. The process model assumes that the local population size in the first year at habitat patch s, denoted $N_{s,1}$, follows a Poisson

292 distribution such that $N_{s,1} \sim Poisson\left(\lambda_s^{[0]}\right)$, in which $\lambda_s^{[0]}$ is a function of continuous elevation

293 and stream distance such that:

294 $$log\left(\lambda_s^{[0]}\right) = \beta_0^{[0]} + \beta_1^{[0]} \times ELE_s + \beta_2^{[0]} \times STR_s + \beta_3^{[0]} \times ELE_s \times STR_s + \varepsilon_s^{[0]} \quad (10)$$

295 which the residuals $\varepsilon_s^{[0]}$ follow a Normal distribution with mean 0 and standard deviation $\sigma^{[0]}$.

296 For subsequent years, the model assumes that variation in local population sizes are a

297 consequence of demographic processes including survival, reproduction, immigration, and

298 emigration, and thus have $N_{s,t} = R_{s,t} + S_{s,t} - E_{s,t} + I_{s,t}$, where $R_{s,t}$ is the number of individuals

299 that are reproduced in habitat patch s and year t, $S_{s,t}$ is the number of individuals in habitat patch

300 s that survived from year t-1 to t, $E_{s,t}$ is the number of individuals that emigrated from habitat

301 patch s in year t, and $I_{s,t}$ is the number of individuals that immigrated into habitat patch s in year

302 t. We further assumed that $R_{s,t}$ follows a Poisson distribution such that $R_{s,t} \sim Poisson(N_{s,t-1} \times$

303 $\gamma_{s,t-1})$, in which the per capita reproduction rate $\gamma_{s,t-1}$ is a function of local population size,

304 elevation and stream distance such that:

305 $$log(\gamma_{s,t}) = \beta_0^{[R]} + \beta_1^{[R]} \times \left(N_{s,t} - \lambda_s^{[0]}\right)/\lambda_s^{[0]} + \beta_2^{[R]} \times ELE_s + \beta_3^{[R]} \times STR_s + \beta_4^{[R]} \times ELE_s \times STR_s + \varepsilon_{s,t}^{[R]} \quad (11)$$

306 which the residuals $\varepsilon_{s,t}^{[R]}$ follows a Normal distribution with mean 0 and standard deviation $\sigma^{[R]}$.

307 We assumed that $S_{s,t}$ follows a Binomial distribution such that

308 $S_{s,t} \sim Binomial(N_{s,t-1}, \omega_{s,t-1})$, in which the survival probability $\omega_{s,t-1}$ is a function of local

309 population size, elevation and stream distance:

310 $$log(\omega_{s,t}) = \beta_0^{[S]} + \beta_1^{[S]} \times \left(N_{s,t} - \lambda_s^{[0]}\right)/\lambda_s^{[0]} + \beta_2^{[S]} \times ELE_s + \beta_3^{[S]} \times STR_s + \beta_4^{[S]} \times ELE_s \times STR_s + \varepsilon_{s,t}^{[S]} \quad (12)$$

311 which the residuals $\varepsilon_{s,t}^{[S]}$ follows a Normal distribution with mean 0 and standard deviation $\sigma^{[S]}$.

We further assumed that $E_{s,t}$followed a Binomial distribution such that:

$$E_{s,t} \sim Binomial(S_{s,t}, \kappa) \quad (13)$$

in which κ is the probability of emigration given that an individual survived. Immigrant individuals are assumed to be emigrants from other patches, and the number of immigrants was calculated as

$$I_{s,t} = \sum_{j=1}^{n} M_{j,s,t} \quad (14)$$

where $M_{j,s,t}$is the number of individuals that moved from grid *j* to grid *s* at year *t* and follows a Multinomial distribution such that $M_{j,s,t} \sim Multinomial(E_{j,t}, w_{j,s})$. The movement rate between grid cells *j* and *s* is a function of the distance between the centroids of these two grids ($d_{j,s}$):

$$w_{j,s} = \exp\left(-\theta \times d_{j,s} + \varepsilon_{j,s}^{[M]}\right) \Big/ \sum_{s=1}^{n} \exp\left(-\theta \times d_{j,s} + \varepsilon_{j,s}^{[M]}\right) \quad (15)$$

where θ is the decay parameter and the error term $\varepsilon_{j,s}^{[M]}$ follows a Normal distribution with mean 0 and standard deviation $\sigma^{[M]}$.

The observation model assumes that the age-structured counts are generated for adults and juveniles separately without individual identification. Counts for adults at site *s* and year *t* during survey *k* informs local populations $N_{s,t}$such that $Y_{s,t,k}^{[a]} \sim Binomial(N_{s,t}, p_t^{[obs]})$, and counts for juveniles informs $R_{s,t}$ such that $Y_{s,t,k}^{[j]} \sim Binomial(R_{s,t}, p_t^{[obs]})$, in which the detection probability $p_t^{[obs]}$ is a random effect such that $logit\left(p_t^{[obs]}\right)$ follows a Normal distribution with mean $\mu^{[obs]}$ and standard deviation $\sigma^{[obs]}$. We included an offset term (search area/100 m^2) in both the adult and juvenile observation sub-model to accout for variable number of count plots in each 100m^2 grid. The capture-recapture process also assumes a capture probability $p_t^{[cap]}$ which

again is a random effect such that $logit\left(p_t^{[cap]}\right)$ follows a Normal distribution with mean $\mu^{[cap]}$ and standard deviation $\sigma^{[cap]}$. The likelihood of the individual encounter history is based on $\omega_{s,t}$, κ, $w_{j,s}$, and $p_t^{[cap]}$.

We used vague normal priors for all covariates with a mean of 0 and precision of 0.01. We fit the model in JAGS (Plummer 2003) using *jagsUI* (Kellner 2017). Following a burn in of 2,500 and adaptation phase of 5,000, 15 MCMC chains were run for 35,000 iterations, thinned at a rate of 15 for a total posterior sample of 30,495. Fully annotated code for each of the above-described models can be found at https://github.com/meaghanregina/Plethodon-IPM-SCJS. For all estimates and covariates we considered support for the direction of the effect to be meaningful if >85% of the posterior density was to one side of zero.

Results

Across 15 surveys over 4 years, we captured a total of 2,310 salamanders representing six species (*Desmognathus occoee, D. monticola, D. quadramaculatus, D. wrighti, Eurycea wilderae*, and *Plethodon shermani*), among which 532 (23.0%) were recaptured. We captured 1,712 individuals of the target species, *P. shermani,* recapturing 447 animals at least once (range: 1–6; 26.1% recapture rate). The average SVL of all *P. shermani* captured was 53.66 mm (range: 20.83 – 77.70 mm). The average SVL for adult females across all sites was 59.31 mm (range: 37.15 – 77.70) and adult males was 57.98 (range: 40.24 – 74.45). Out of 753 animals captured and photographed across the 6 low elevation sites, 730 (97.50%) exhibited some level of visible hybrid traits, with the other animals being pure *P. teyahalee.* No high elevation animals exhibited combined hybrid traits of spotting and red-legs, but there was variation in the amount of red present on legs.

356 *Growth Model* — Salamanders from high elevations had higher growth rates (*K*) (mean:
357 0.561, 95% CRI: 0.477, 0.652) than those from low elevation (mean: 0.457, 95% CRI: 0.387,
358 0.536) (Table 1). There was a negative effect of distance from stream on growth at high
359 elevations (mean: -0.034, 95% CRI: -0.066, -0.004) but the effect of stream distance was positive
360 at low elevation (mean = 0.020, 95% CRI: -0.011, 0.055). There was also a positive effect of
361 precipitation at both high (mean = 0.209, 95% CRI: 0.102, 0.320) and low elevations (mean =
362 0.063 95% CRI: -0.022, 0.149) on growth. At low elevations, animals with more hybrid
363 characteristics had reduced growth (mean = -0.015, 95% CRI: -0.048, 0.016), Salamanders at
364 high elevation reached a lower asymptotic size (66.01 mm, 95% CRI: 64.28, 67.85) than those at
365 low elevations (73.52 mm, 95% CRI: 71.65, 75.50) (Table 1). The mean estimated age of
366 maturity at high elevation is 1.81 years (95% CRI: 1.77, 1.84) and for low elevation hybrids is
367 2.02 years (95% CRI: 1.98, 2.12) (Fig. 2).
368 *sCJS* –Across our survey period, the average annual survival of salamanders was 0.595
369 (95% CRI: 0.508, 0.694) at high elevation and 0.874 (95% CRI: 0.744, 1.00) at low elevations.
370 At high elevation, there was no effect of stream distance on survival (mean = 0.056, 95% CRI: -
371 0.498, .516) and stream distance had a negative but marginal effect on survival at low elevations
372 (mean = -1.046, 95% CRI: -9.773, 3.15). At low elevations, animals with more hybrid
373 characteristics had increased survival probability (mean = -3.016, 95% CRI:-7.543,-0.652) (Fig.
374 3A) and decreased movement probability (mean: 1.216, 95% CRI: 0.796, 1.641) (Fig. 3C). At
375 high elevations, more 'pure' *P. shermani* had increased survival probability (mean = 1.160, 95%
376 CRI:-0.058,2.605) (Fig. 3B) and decreased movement probability (mean: -0.635, 95% CRI: -
377 0.866, -0.294) (Fig. 3D). Salamanders from high elevation had a mean movement of 1.822 m
378 (95% CRI: 0.058, 6.504) while those at low elevation had a mean movement of 3.323 m (95%

CRI: 0.107, 12.001) (Fig. 4A). There was greater variance in movement at low elevations (10.341; 95% CRI: 6.966, 14.831) than high elevations (3.113, 95% CRI: 2.579, 3.794) (Fig. 4B). The distance from stream had a marginally negative effect on movement at high elevation (-0.082, 95% CRI: -0.233, 0.062) but a substantial positive effect at low elevation (0.320, 95% CRI: -0.038, 0.681) (Fig. 4A). The average individual recapture probability across all sites was 0.157 and recapture was positively influenced by relative humidity and surface soil temperature and negatively influenced by air temperature (Supporting Information Figure 2)

SEIPM –Our models show that initial population size increased with elevation (mean = 0.529, 95% CRI: 0.305, 0.749) and decreased with the distance from stream (mean = -0.118, 95% CRI: -0.362, 0.128) without an interaction between elevation and stream distance (mean = 0.018, 95% CRI: -0.255, 0.277). The average survival across all sites was 0.432 (95% CRI: 0.315, 0.513) and was not density dependent (mean = 0.175, 95% CRI: -1.877, 1.903). There was a significant negative interaction between elevation and stream distance on survival, meaning that survival was highest at low elevation near streams and declined with the distance from stream at low elevations (Fig. 5). Per capita reproduction averaged 0.249 (95% CRI: 0.153, 0.421) across the landscape and was negatively influenced by population density (mean = -0.966, 95% CRI: -1.793, -0.209). There was also a significant positive interaction between elevation and stream distance on per capita reproduction rate whereby reproduction increases with elevation and at low elevation, reproduction decreases with stream distance (Fig. 6). Emigration probabilities were low (mean = 0.014, 95% CRI: 0.001, 0.073), indicating a low probability that an individual will move from their 100-m grid cell; however, a low value of the decay parameter in dispersal (mean = 0.006, 95% CRI: 0.001, 0.005) indicated that individual moved a long

401 distance if they dispersed. The average detection probability for animals across all count plots
402 was 0.270 and average recapture probability across all sMRC sites was 0.338.
403
404 **Discussion**
405 Estimating demographic variation in populations across space provides insight into the
406 role that landscape heterogeneity plays in driving ecological processes (Gurevitch et al. 2016).
407 Using elevation and stream distance as proxies for temperature and moisture variation, we reveal
408 nuanced spatial patterns in population demography as well as how demographic rates at a fine
409 scale have consequences for species performance at broader landscape scales. We show that
410 spatial heterogeneity of microhabitats drives demographic rates such that growth rates,
411 movement, and survival are highest at low elevations and both growth and movement increase
412 with stream distance at low elevation. High elevation salamanders grow faster and reach maturity
413 approximately two and half months earlier than low elevations animals, but low elevation
414 animals reach a larger size. The larger sizes at low elevation is likely attributed to the larger
415 hatchling sizes of hybrid animals. Hairston (1983) similarly noted that *P. jordani* (a closely
416 related species to *P. shermani*) and *P. teyahalee* populations had similar size distributions at all
417 ages, but *P. teyahalee* reached a larger maximum size. Interestingly, our estimates for age at
418 maturity across elevations were lower than previous estimates (Hairston 1982; Connette 2014),
419 which may be attributed to the environmental conditions both preceding and during surveys.
420 Precipitation drives higher growth rates (Caruso & Rissler, 2018; Connette, Crawford, &
421 Peterman, 2015) but, large adult *P. shermani* appear to be disproportionately active under drier
422 conditions which may introduce sampling bias in growth and maturity estimates (Connette et al.,
423 2015).

Our results also suggest that precipitation has a much larger effect on growth at high elevations than low elevations (Table 1). Relative to *P. shermani, P. teyahalee* are larger bodied and subsequently have higher resistance to water loss (Riddell & Sears, 2015). With greater resistance to water loss, larger hybrid animals may have less reliance on precipitation for growth (Table 1). Given our model estimates and previous work (Caruso et al., 2020; Caruso & Rissler, 2018; Connette et al., 2015), precipitation influences growth rates more strongly than spatial variation in moisture or temperature which could have significant demographic consequences including increases annual growth rates variability leading to changes in time to maturity, reduced lifetime fecundity, and changes in population size structures in the future, especially considering the increased variability in precipitatation by the end of the century in the Southern Appalachian region (Kunkel et al. 2020).

Terrestrial plethodontid salamanders are known to have small home ranges and limited dispersal capacity of less than 3 m (Cabe et al., 2007; Caruso & Rissler, 2018; Muñoz et al. 2016). We found that *Plethodon* has low dispersal across the landscape as a whole, but *P. shermani* from high elevations move less and with less variation than low elevation animals. Increased variation in movement at low elevations may be attributed to hybrid animals considering hybrids moved less than more 'pure' *P. shermani* (Fig. 3) and more broadly, movement rates are likely tied to temperature. Low elevations are warmer than high elevations, especially far from streams, where we estimated increased movement probability (Fig 4A) (Gade & Peterman 2019). Temperature appears to increase surface activity probability in *Plethodon* (Gade et al. 2020), other salamander families (Johnson, Johnson, & Shaffer, 2010), and other ectotherms like lizards and fish (Xiang et al. 1996, Petty et al. 2012) potentially as a result of increased metaboic demands. As such, more surface activity dedicated to nutrient acquisition is

likely required to offset the metabolic costs associated with low elevation and far from stream habitats. Increased movement for nutrient acquisition may come at a cost to reproductive effort, a pattern we observed in animals at low elevations (Fig. 6). Movement may also be tied to resources availability (poorer quality prey at low eleavtions) or population density: decreased population density at low elevations may lead to intraspecific competitive release and increased movement probability (Gade & Peterman 2019).

Our SEIPM estimated that annual *P. shermani* survival probability decreased with elevation. Caruso and Rissler (2018) described similar elevational trends in survival in a closely related species, *P. montanus* and showed survival was positively associated with temperature. Temperature appears to be linked with higher energy assimilation and survival rates, but only to an optimal temperature, which when surpassed, rates decline rapidly (Caruso & Rissler, 2018; Clay & Gifford, 2018a). In our system, we see further evidence for this relationship whereby survival probability dropped to 0.19 in animals found at low elevations and far from streams (Fig. 5). Temperature increases and humidity decreases with stream distance at low elevations (Gade & Peterman, 2019), creating high vapor pressure deficits that exacerbate water loss and provide unsuitable conditions for terrestrial salamanders (Peterman & Gade, 2017; Riddell, Apanovitch, Odom, & Sears, 2017). The hot and dry conditions far from streams provide a combination of abiotic stressors that salamanders may not be able to survive. For example, Gade (2021) found that salamanders can compensate hormonal stress responses to one environmental stressor (e.g. temperature), but are overwhelmed by multiple abiotic stressors (e.g. temperature and lack of moisture). Thus, multiple environmental stressors appear to significantly impact the overall fitness of animals. Although our SEIPM suggests a strong positive effect of stream distance on survival at high elevations (Fig. 5), this trend is due to increased uncertainty in model

estimates (Supplemental Fig. 4) as these regions were not well sampled due to logistical constraints (Gade & Peterman, 2019)

Per capita reproduction increases with elevation (Fig. 6) and may be a contributing factor to the positive association between elevation and abundance patterns observed in Gade and Peterman (2019). In a related *Plethodon* spp., population growth rates were lowest at low elevations, aligning with our reduced reproductive rate estimates (Caruso et al., 2020). Higher reproductive rates at high elevations may also serve as a compensatory mechanism for the lower estimated survival probability at high elevations (Muths et al. 2011; Villellas et al. 2015; Buckley et al. 2021). Negative covariance between vital rates can occur to maintain demographic performance over environmental gradients. Such demographic compensation between reproduction and survival may contribute to local adaptation to environmental conditions (Angilletta et al, 2003) and we observed other vital rates that may contribute to energy tradeoffs and local adaptation across temperature and moisture gradients. For example, since low elevation animals experience warmer temperatures and higher metabolic demands (Clay and Gifford 2018b), individuals must remain surface active to obtain the necessary resources for growth potentially at the cost to reproductive output. Conversely, at high elevations animals move less while still maintaining equal growth rates allowing for greater investment into reproduction. Further, lungless salamanders must constantly regulate and invest energy into water loss resistance, which is achieved through capillary bed regeneration or regression (Riddell, Roback, Wells, Zamudio, & Sears, 2019). With low elevation animals moving more and experiencing higher desiccation probability, there is likely a significant amount of energy diverted from reproduction and invested into water loss resistance for survival purposes. Alternatively, at high elevations where conditions are broadly cooler and wetter, there may be less energy budgeted to

493 water loss regulation, allowing energy investment into reproduction. We also observed both
494 reproduction and survival rates declining with stream distance at low elevations (Figs 5, 6)
495 suggesting the hot and dry conditions in these habitats surpass any ability of salamanders to
496 maintain vital rates. The complex spatial patterns of vital demographic rates provide valuable
497 insight into compensations between life-history and energy allocation across a landscape with
498 multiple abiotic gradients.

499 Our study focuses on the spatial variation in demographic rates across abiotic gradients
500 that represent the range of environmental conditions experienced by individuals. This spatial
501 approach offers an understanding into the role of abiotic gradients on demography but neglects
502 the temporal aspect of demographic rates. Due to the somewhat limited timescale of our study (4
503 years) especially relative to the lifespan of *Plethodon* (~10 years; Staub, 2016), we do not
504 capture enough temporal variation to make robust estimates. Demographic rates are influenced at
505 different time scales. For example, survival is often affected by short term exposure to extreme
506 environmental conditions whereas fecundity and reproduction tend to be an integrated response
507 to longer-term environmental stochasticity (Levins 1968; Gilchrist 1995; Buckley et al. 2021).
508 While our present study, to some extent, substitutes space-for-time to understand how
509 temperature and moisture gradients influence population vital rates at individual plot-levels as
510 well as across the entire landscape, we are limited in our inference of how stochasticity in
511 weather events (i.e., droughts, heat waves) affect vital rates in the long term. Continued
512 monitoring of these populations will be necessary to disentangle temporal effects on
513 demography.

514 Hybridization may allow species to survive in rapidly changing environments by
515 promoting phenotypic and genotypic novelty more quickly than typical evolutionary mechanisms

516 (Arnold 1997; Rieseberg et al. 2003). In our study, hybrid individuals at low elevations had a
517 higher survival probability than non-hybrid, "pure" *P. shermani* (Fig. 3A). Hybridization
518 between populations adapted to diminishing abiotic environments and those preadapted to
519 emerging environments offers a unique avenue for species to survive climate change (Chunco
520 2014). The warmer temperatures expected with climate change in the future may particularly
521 benefit hybrid *P. shermani* because *P. teyahalee* are preadapted to occupy warmer and drier
522 microhabitats (Hairston et al., 1992), and larger bodied salamanders have higher resistance to
523 water loss. However, *P. teyahalee* tend to occupy warmer but moist microhabitats that minimize
524 water loss (Farallo et al. 2020), which may potentially balance the costs of higher temperatures.
525 Our survival estimates decline with stream distance at low elevation, where temperatures are
526 high and humidity is low, a microhabitat that appears unsuitable even for hybrid individuals.
527 Thus, hybridization may only be beneficial if moist microhabitats are maintained in the future.
528 Contemporary hybridization may facilitate Plethodontid diversification through increased
529 speciation and decreased extinction rates (Patton et al. 2020), and may be a creative strategy for
530 rapid adaptation to novel stressors expected with climate change. It will be critical to continue
531 monitoring hybrid populations for greater resolution of the role hybridization may play in
532 salamanders.

533 Our study demonstrates that demographic estimates can vary by the scale at which they
534 are assessed. Robustly sampled fine-scale estimates provide valuable information but may not
535 necessarily represent landscape-scale patterns. We show that data sources measured at different
536 scales can be combined to estimate nuanced spatial variation in critical demographic rates across
537 a heterogenous landscape and highlights the need for future studies to evaluate vital rates and life
538 history across relevant environmental gradients. Estimation of landscape-scale demographic rates

has previously been limited by time, costs, and logistics. SEIPMs provide a rigorous and coherent framework for maximally leveraging disparate data sources and a promising tool for future spatial demographic studies.

Acknowledgements

We thank the many people who contributed to field collection including Philip Gould, Katie Greene, Addison Hoven, Andrew Wilk, Nicole Cooke, Winter Gary, Kate Donlon, Amelia Gray, and Kasey Foley. We also thank members of the Peterman Lab group, Suzanne Gray, Lauren Pintor, and Chris Tonra for helpful comments on earlier version on the manuscript. We also thank the staff at Highlands Biological Station for their logistical support.

Declarations

Funding: This work was supported by The Herpetologists League E.E. Williams grant and multiple Grant-in-aids from Highlands Biological Station.

Conflicts of Interest: The authors have no conflicts of interest to declare.

Ethics Approval: This research was conducted following The Ohio State University IACUC protocol #2016A00000026, with permission from the US Forest Service Permit number NAN 45716.

Consent to Participate: NA

Consent for publication: NA

Availability of data and material: All data is available on GitHub link: https://github.com/meaghanregina/Plethodon-IPM-SCJS

Code Availability: Code is available on GitHub: https://github.com/meaghanregina/Plethodon-IPM-SCJS

Author Contributions: MRG and WEP conceived the ideas and designed the methodology. MRG collected the data. MRG and QZ analyzed the data and MRG lead the writing of the manuscript. All authors contributed equally to drafts of the manuscript and have given final approval for publication.

568 **Literature Cited**

569 Arnold M (1997) Natural Hybridization and evolution. Oxford University Press, Oxford

570 Bailey LL (2004) Evaluating elastomer marking and photo identification methods for terrestrial
571 salamanders: marking effects and observer bias. Herpetol Rev 38–41

572 Blaustein AR, Han BA, Relyea RA, et al (2011) The complexity of amphibian population
573 declines: Understanding the role of cofactors in driving amphibian losses. Ann N Y Acad
574 Sci 1223:108–119. doi: 10.1111/j.1749-6632.2010.05909.x

575 Brown JH, Kodric-Brown A (1977) Turnover Rates in Insular Biogeography : Effect of
576 Immigration on Extinction. Ecology 58:445–449

577 Buckley LB, Schoville SD, Williams CM (2021) Shifts in the relative fitness contributions of
578 fecundity and survival in variable and changing environments. J Exp Biol 224:. doi:
579 10.1242/jeb.228031

580 Cabe PR, Page RB, Hanlon TJ, et al (2007) Fine-scale population differentiation and gene flow
581 in a terrestrial salamander (Plethodon cinereus) living in continuous habitat. Heredity
582 (Edinb) 98:53–60. doi: 10.1038/sj.hdy.6800905

583 Caruso N, Rissler LJ (2018) Demographic consequences of climate variation along an
584 elevational gradient for a montane terrestrial salamander. Popul Ecol 1–12. doi:
585 10.1002/1438-390X.1005

586 Caruso NM, Staudhammer CL, Rissler LJ (2020) A demographic approach to understanding the
587 effects of climate on population growth. Oecologia 193:889–901. doi: 10.1007/s00442-020-
588 04731-8

589 Chunco AJ (2014) Hybridization in a warmer world. Ecol Evol 4:2019–2031. doi:
590 10.1002/ece3.1052

591 Chunco AJ, Jobe T, Pfennig KS (2012) Why do species co-occur? a test of alternative
592 hypotheses describing abiotic differences in sympatry versus allopatry using spadefoot
593 toads. PLoS One 7:. doi: 10.1371/journal.pone.0032748
594 Clay TA, Gifford ME (2018a) Energy Assimilation in a Polymorphic Salamander, Plethodon
595 angusticlavius. Source J Herpetol 52:269–272. doi: 10.1670/17-140
596 Clay TA, Gifford ME (2018b) Thermal constraints of energy assimilation on geographical
597 ranges among lungless salamanders of North America. J Biogeogr 45:1664–1674. doi:
598 10.1111/jbi.13347
599 Connette G (2014) Individual, Population and Landscape-scale effecs of timber harvest on the
600 red-legged salamander (Plethodon shermani). Dissertation 1–126
601 Connette GM, Crawford JA, Peterman WE (2015) Climate change and shrinking salamanders:
602 alternative mechanisms for changes in plethodontid salamander body size. Glob Chang Biol
603 21:2834–2843. doi: 10.1111/gcb.12883
604 Elsen PR, Tingley MW (2015) Global mountain topography and the fate of montane species
605 under climate change. Nat Clim Chang 5:772–776. doi: 10.1038/nclimate2656
606 Fabens AJ (1965) Properties and fitting of the Von Bertalanffy growth curve. Growth 29:265–
607 289
608 Farallo VR, Muñoz MM, Uyeda JC, Miles DB (2020) Scaling between macro- to microscale
609 climatic data reveals strong phylogenetic inertia in niche evolution in plethodontid
610 salamanders. Evolution (N Y) 74:979–991. doi: 10.1111/evo.13959
611 Feder ME, Londos PL (1984) Hydric Constraints upon Foraging in a Terrestrial Salamander,
612 Desmognathus ochrophaeus. Oecologia 64:413–418
613 Ficke AD, Myrick CA, Hansen LJ (2007) Potential impacts of global climate change on

freshwater fisheries. Rev Fish Biol Fish 17:581–613. doi: 10.1007/s11160-007-9059-5

Gade MR (2021) Spatial variation in the abundance, demography, and physiology of the montane endemic salamander, Plethodon shermaini, and teh consequences of climate change. The Ohio State University

Gade MR, Peterman WE (2019a) Multiple environmental gradients influence the distribution and abundance of a key forest-health indicator species in the Southern Appalachian Mountains, USA. Landsc Ecol

Gade MR, Peterman WE (2019b) Multiple environmental gradients influence the distribution and abundance of a key forest-health indicator species in the Southern Appalachian Mountains, USA. Landsc Ecol 34:569–582. doi: 10.1007/s10980-019-00792-0

Garroway CJ, Bowman J, Cascaden TJ, et al (2010) Climate change induced hybridization in flying squirrels. Glob Chang Biol 16:113–121. doi: 10.1111/j.1365-2486.2009.01948.x

Gilchrist GW (1995) Specialists and generalists in changing environments. I. Fitness landscapes of thermal sensitivity. Am Nat 146:252–270. doi: 10.1086/285797

Grant EHC, Miller D, Schmidt B, et al (2016) Quantitative evidence for the effects of multiple drivers on continental-scale amphibian declines. Sci Rep 6:25625

Gurevitch J, Fox GA, Fowler NL, Graham CH (2016) Landscape demography: Population change and its drivers across spatial scales. Q Rev Biol 91:459–485. doi: 10.1086/689560

Hairston NG (1983) Growth , Survival and Reproduction of Plethodon jordani : Trade-Offs between Selective Pressures. Copeia 4:1024–1035

Hairston NG, Wiley RH, Smith CK, Kneidel KA (1992) The dynamics of two hybrid zones in Appalachian salamanders of the genus Plethodon. Evolution (N Y) 46:930–938. doi: 10.1111/j.1558-5646.1992.tb00610.x

637 Highton R (1962) Geographic variation in the life history of the slimy salamander. Copeia 597–
638 613
639 Highton R, Peabody RB (2000) Geographic Protein Variation and Speciation in Salamanders of
640 the Plethodon Jordani and Plethodon Glutinosus Complexes in the Southern Appalachian
641 Mountains with the Description of Four New Species. In: The Biology of Plethodontid
642 Salamanders. Springer US, pp 31–93
643 Hocking D, Babbitt K (2014) Amphibian contributions to ecosystem services. Herpetol Conserv
644 Biol 9:1–17
645 Johnson JR, Johnson BB, Bradley Shaffer H (2010) Genotype and temperature affect locomotor
646 performance in a tiger salamander hybrid swarm. Funct Ecol 24:1073–1080. doi:
647 10.1111/j.1365-2435.2010.01723.x
648 Kellner K (2017) jagsUI: a wrapper around 'rjags' to streamline 'JAGS.' R package version
649 1.4.9
650 Kunkel KE, Easterling DR, Ballinger A, et al (2020) North Carolina Climate Science Report
651 Levins R (1968) Evolution in Changing Environments. Princeton Universtiy Press
652 MacLean SA, Beissinger SR (2017) Species' traits as predictors of range shifts under
653 contemporary climate change: A review and meta-analysis. Glob Chang Biol 23:4094–
654 4105. doi: 10.1111/gcb.13736
655 Marshall MR, Diefenbach DR, Wood LA, Cooper RJ (2004) Annual survival estimation of
656 migratory songbirds confounded by incomplete breeding site-fidelity: Study designs that
657 may help. Anim Biodivers Conserv 27:59–72
658 Muñoz DJ, Hesed KM, Grant EHC, Miller DAW (2016) Evaluating within-population variability
659 in behavior and fitness for the climate adaptive potential of a dispersal-limited species,

660 Plethodon cinereus. Ecol Evol 1–16. doi: 10.1002/ece3.2573
661 Muths E, Scherer RD, Pilliod DS (2011) Compensatory effects of recruitment and survival when
662 amphibian populations are perturbed by disease. J Appl Ecol 48:873–879. doi:
663 10.1111/j.1365-2664.2011.02005.x
664 Oropeza–Sánchez MT, Sandoval–Comte A, García–Bañuelos P, et al (2020) Use of visible
665 implant elastomer and its effect on the survival of an endangered minute salamander. Anim
666 Biodivers Conserv 43:187–190. doi: 10.32800/abc.2020.43.0187
667 Patton AH, Margres MJ, Epstein B, et al (2020) Hybridizing salamanders experience accelerated
668 diversification. Sci Rep 10:1–12. doi: 10.1038/s41598-020-63378-w
669 Peterman WE, Gade M (2017) The importance of assessing parameter sensitivity when using
670 biophysical models: a case study using plethodontid salamanders. Popul Ecol. doi:
671 10.1007/s10144-017-0591-4
672 Plummer M (2003) JAGS: A program for analysis of Bayesian graphical models using Gibbs
673 sampling. In: Proceedings of the 3rd International Workshop on Distributed Statistical
674 Computing (DSC2003). pp 20–22
675 Reid JM, Bignal EM, Bignal S, et al (2006) Spatial variation in demography and population
676 growth rate: The importance of natal location. J Anim Ecol 75:1201–1211. doi:
677 10.1111/j.1365-2656.2006.01143.x
678 Riddell E, Roback E, Wells C, et al (2019) Thermal cues drive plasticity of desiccation resistance
679 in montane salamanders with implications for climate change. Nat Commun 10:. doi:
680 10.1017/cbo9781316105542.007
681 Riddell E, Sears MW (2015) Geographic variation of resistance to water loss within two species
682 of lungless salamanders : implications for activity. Ecosphere 6:1–16. doi: 10.1890/ES14-

683 00360.1
684 Riddell EA, Apanovitch EK, Odom JP, Sears MW (2017) Physical calculations of resistance to
685 water loss improve predictions of species range models. Ecol Monogr 87:21–33. doi:
686 10.1002/ecm.1240
687 Riddell EA, Iknayan KJ, Hargrove L, et al (2021) Exposure to climate change drives stability or
688 collapse of desert mammal and bird communities. Science (80-) 371:633 LP – 636. doi:
689 10.1126/science.abd4605
690 Rieseberg LH, Raymond O, Rosenthal DM, et al (2003) Major ecological transitions in wild
691 sunflowers facilitated by hybridization. Science (80-) 301:1211–1216. doi:
692 10.1126/science.1086949
693 Schaub M, Abadi F (2011) Integrated population models: A novel analysis framework for deeper
694 insights into population dynamics. J Ornithol 152:S227–S237. doi: 10.1007/s10336-010-
695 0632-7
696 Schaub M, Royle JA (2014) Estimating true instead of apparent survival using spatial Cormack-
697 Jolly-Seber models. Methods Ecol Evol 5:1316–1326. doi: 10.1111/2041-210X.12134
698 Seehausen O (2004) Hybridization and adaptive radiation. Trends Ecol Evol 19:198–207. doi:
699 10.1016/j.tree.2004.01.003
700 Staub NL (2016) The Age of Plethodontid Salamanders: A Short Review on Longevity. Copeia
701 104:118–123. doi: 10.1643/OT-14-200
702 Sullivan SMP, Vierling KT (2012) Exploring the influences of multiscale environmental factors
703 on the American dipper Cinclus mexicanus. Ecography (Cop) 35:624–636. doi:
704 10.1111/j.1600-0587.2011.07071.x
705 Taylor SA, White TA, Hochachka WM, et al (2014) Climate-mediated movement of an avian

706 hybrid zone. Curr Biol 24:671–676. doi: 10.1016/j.cub.2014.01.069
707 Todd Petty J, Hansbarger JL, Huntsman BM, Mazik PM (2012) Brook trout movement in
708 response to temperature, flow, and thermal refugia within a complex Appalachian
709 riverscape. Trans Am Fish Soc 141:1060–1073. doi: 10.1080/00028487.2012.681102
710 Urban MC, Bocedi G, Hendry AP, et al (2016) Improving the forecast for biodiversity under
711 climate change. Science (80-) 353:aad8466-1-aad8466-9. doi: 10.1126/science.aad8466
712 Valencia-Aguilar A, Cortés-Gómez AM, Ruiz-Agudelo CA (2013) Ecosystem services provided
713 by amphibians and reptiles in Neotropical ecosystems. Int J Biodivers Sci Ecosyst Serv
714 Manag 9:257–272. doi: 10.1080/21513732.2013.821168
715 Villellas J, Doak DF, García MB, Morris WF (2015) Demographic compensation among
716 populations: What is it, how does it arise and what are its implications? Ecol Lett 18:1139–
717 1152. doi: 10.1111/ele.12505
718 Walls SC (2009a) The role of climate in the dynamics of a hybrid zone in Appalachian
719 salamanders. Glob Chang Biol 15:1903–1910. doi: 10.1111/j.1365-2486.2009.01867.x
720 Walls SC (2009b) The role of climate in the dynamics of a hybrid zone in Appalachian
721 salamanders. Glob Chang Biol 15:1903–1910. doi: 10.1111/j.1365-2486.2009.01867.x
722 Wiens JA, Stenseth NC, Horne B Van, Ims RA (1993) Ecological Mechanisms and Landscape
723 Ecology. Oikos 66:369. doi: 10.2307/3544931
724 Willis BL, Van Oppen MJH, Miller DJ, et al (2006) The role of hybridization in the evolution of
725 reef corals. Annu Rev Ecol Evol Syst 37:489–517. doi:
726 10.1146/annurev.ecolsys.37.091305.110136
727 Xiang J, Weiguo D, Pingyue S (1996) Body temperature, thermal tolerance and influence of
728 temperature on sprint speed and food assimilation in adult grass lizards, Takydromus

septentrionalis. J Therm Biol 21:155–161. doi: 10.1016/0306-4565(95)00037-2

Zhao Q (2020) On the sampling design of spatially explicit integrated population models. Methods Ecol Evol. doi: 10.1111/2041-210X.13457

Zhao Q, Royle JA, Boomer GS (2017) Spatially explicit dynamic N-mixture models. Popul Ecol 59:293–300. doi: 10.1007/s10144-017-0600-7

736

Table 1. Parameter estimates for the growth model of *P. shermani*. Parenthetical high and low refer to elevation-specific intercept estimates. L is the asymptotic size, K is growth rate. CRI represents credible intervals and f indicates percent of the estimates that lies to one side of zero. Stream distance, hybrid score, and precipitation are continuous covariates of K with elevation-specific estimates.

Parameter	**Mean**	**2.5% CRI**	**97.5% CRI**	**f**
L (High)	66.01	64.38	67.85	1.00
L (Low)	73.51	71.67	75.50	1.00
K (High)	0.56	0.48	0.65	1.00
K (Low)	0.46	0.39	0.54	1.00
Stream (High)	-0.03	-0.07	0.00	0.99
Stream (Low)	0.02	-0.01	0.05	0.89
Hybrid (High)	-0.02	-0.36	0.36	0.54
Hybrid (Low)	0.02	-0.01	0.04	0.84
Precipitation (High)	0.21	0.10	0.32	1.00
Precipitation (Low)	0.06	-0.02	0.15	0.93

737

738

Fig. 1 Locations of the salamander count plots (red circles) and mark-recapture plots (black triangles) on Wayah Mountain in the Nantahala National Forest in western North Carolina.

Fig. 2. Growth projection for high elevation (dotted line) and low elevation (solid line) *P. shermani* based on the growth model. The horizontal lines represent minimum size (in SVL) at maturity for high elevation 'pure' *P. shermani* (blue) and low elevation hybrid *P. shermani* (red).

Fig. 3 The effect of hybrid score on survival probability at (A) low elevations and (B) high elevations and movement probability at (C) low elevations and (D) high elevations from 5000 random draws of the posterior of the sCJS model. Negative hybrid scores indicate more characteristics of *P. teyahalee* and thus represent more hybridization.

Fig. 4 Posterior mean densities for the (A) mean movement distance and stream distance covariates of *P. shermani* and (B) the variance in movement estimated in the sCJS. The parenthetical High and Low refer to the two elevation intercepts estimated. The shaded region indicates 50% of the posterior.

Fig. 5 Interaction between elevation and stream distance on the survival probability of *P. shermani* estimated from the SEIPM. Survival probability is highest at low elevation and decreases with stream distance at lower elevations.

760 **Fig. 6** Interaction between elevation and stream distance on per capita reproduction rate of *P.*
761 *shermani* estimated from the SEIPM. Per capita reproduction increases with elevation and at low
762 elevations, decreases with stream distance.
763

Figures

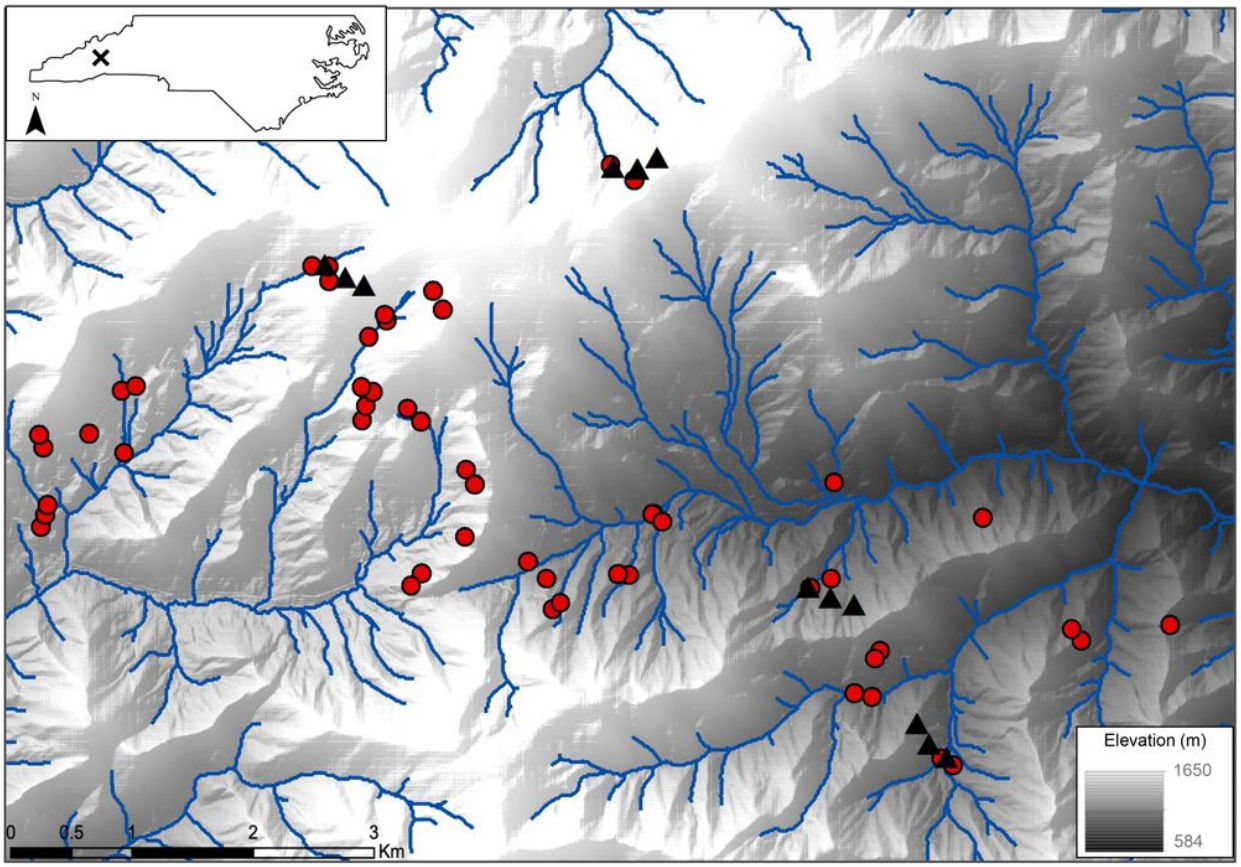

Figure 1

Locations of the salamander count plots (red circles) and mark-recapture plots (black triangles) on Wayah Mountain in the Nantahala National Forest in western North Carolina.

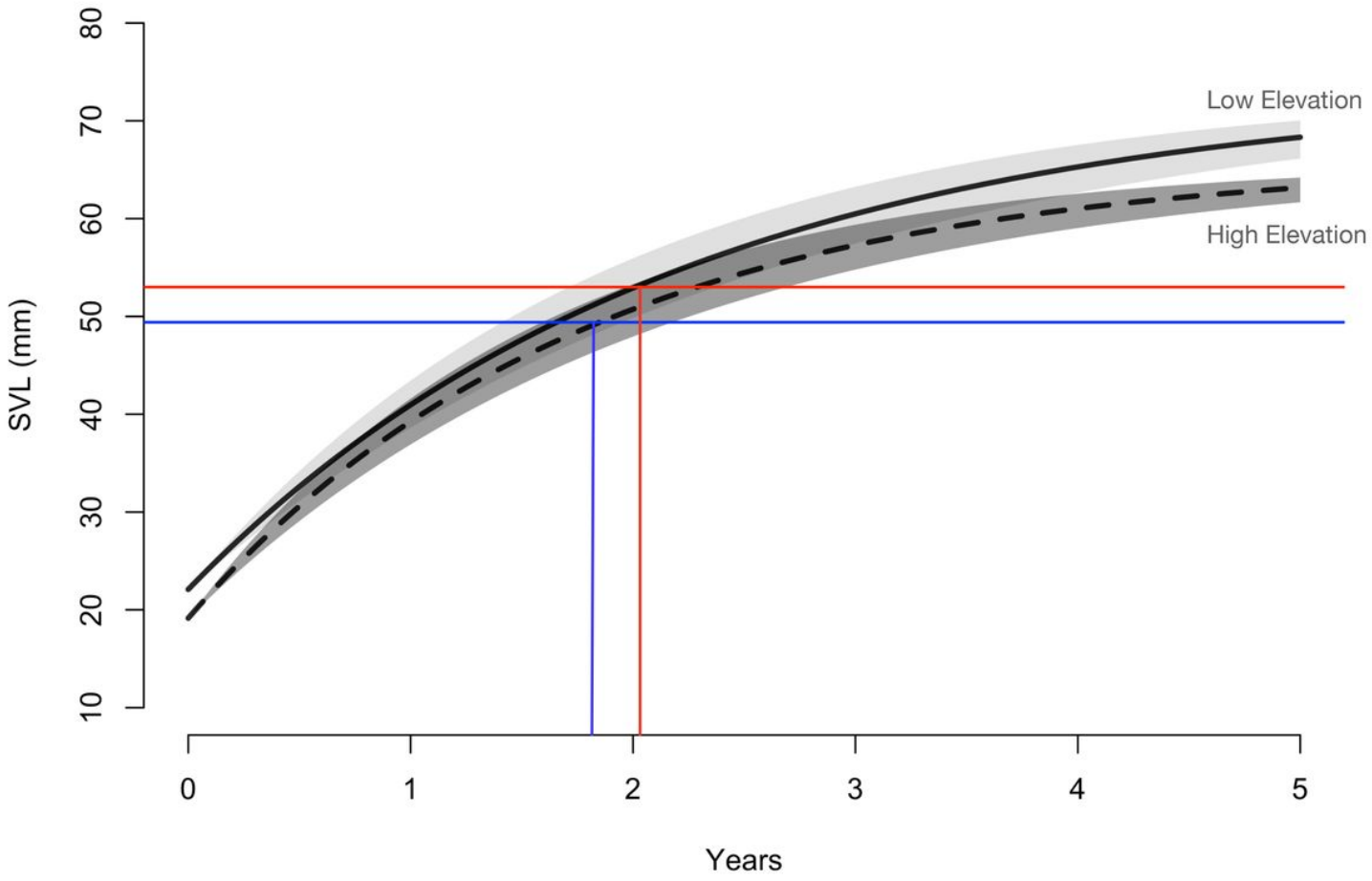

Figure 2

Growth projection for high elevation (dotted line) and low elevation (solid line) P. shermani based on the growth model. The horizontal lines represent minimum size (in SVL) at maturity for high elevation ‘pure’ P. shermani (blue) and low elevation hybrid P. shermani (red).

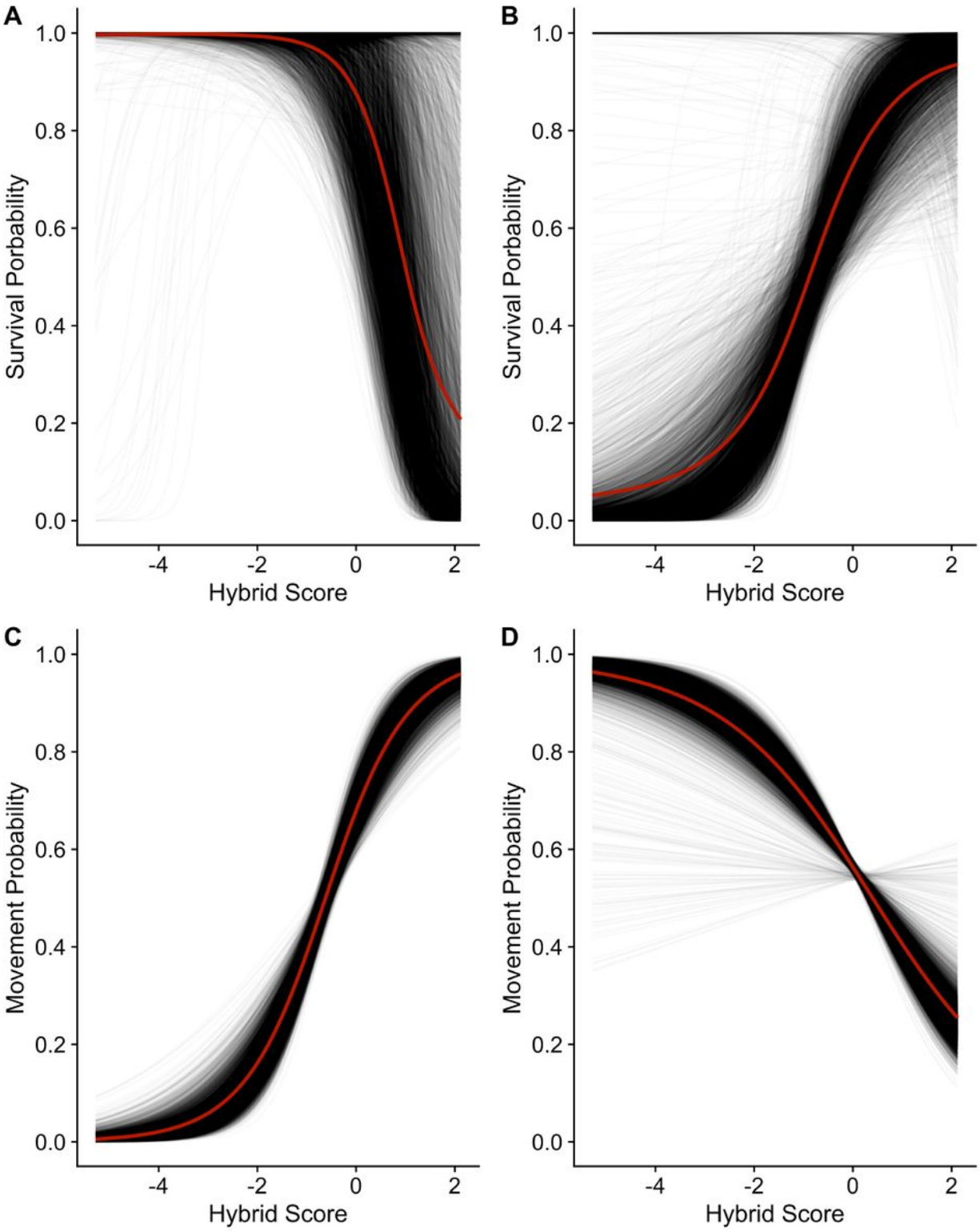

Figure 3

The effect of hybrid score on survival probability at (A) low elevations and (B) high elevations and movement probability at (C) low elevations and (D) high elevations from 5000 random draws of the posterior of the sCJS model. Negative hybrid scores indicate more characteristics of P. teyahalee and thus represent more hybridization.

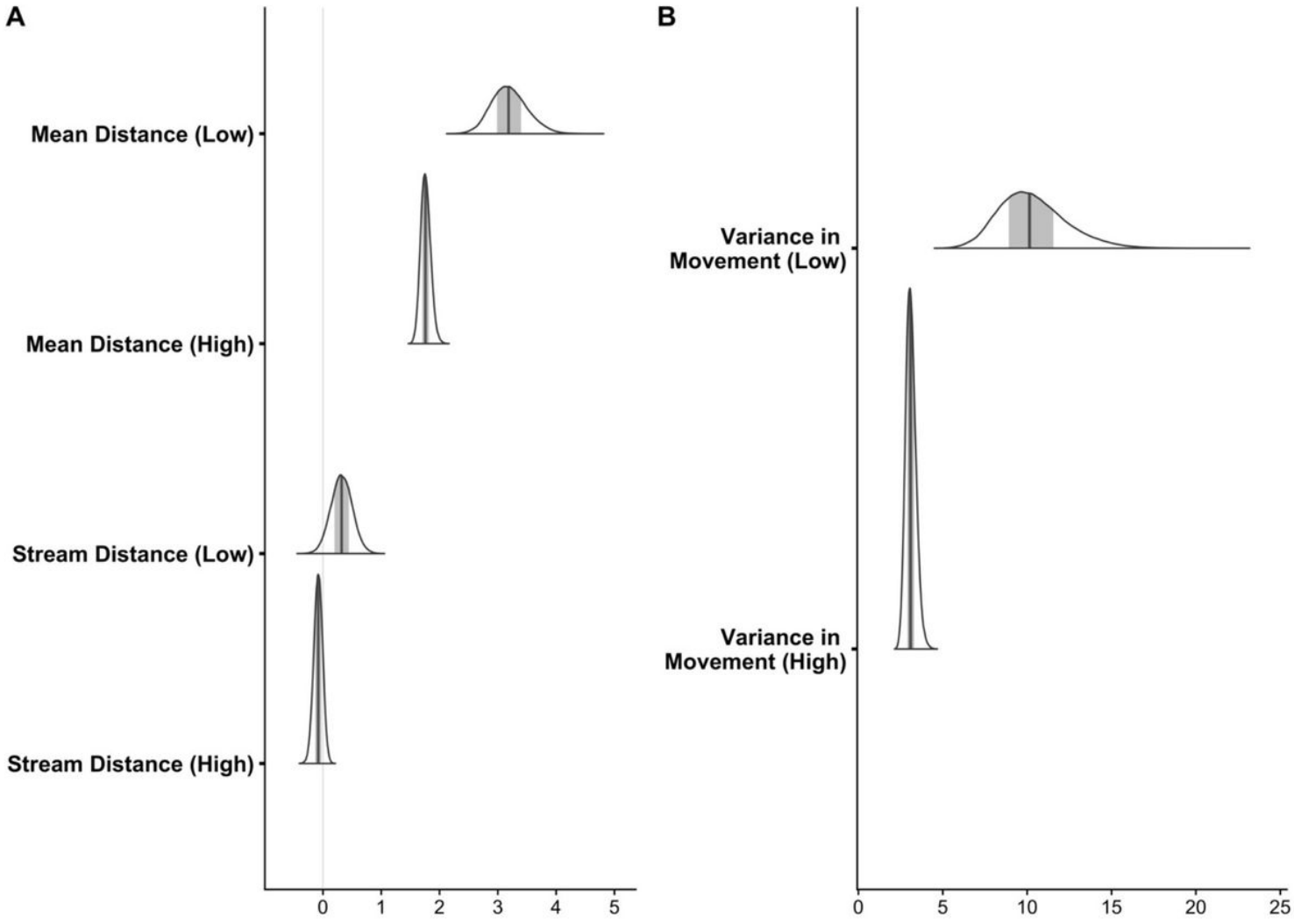

Figure 4

Posterior mean densities for the (A) mean movement distance and stream distance covariates of P. shermani and (B) the variance in movement estimated in the sCJS. The parenthetical High and Low refer to the two elevation intercepts estimated. The shaded region indicates 50% of the posterior.

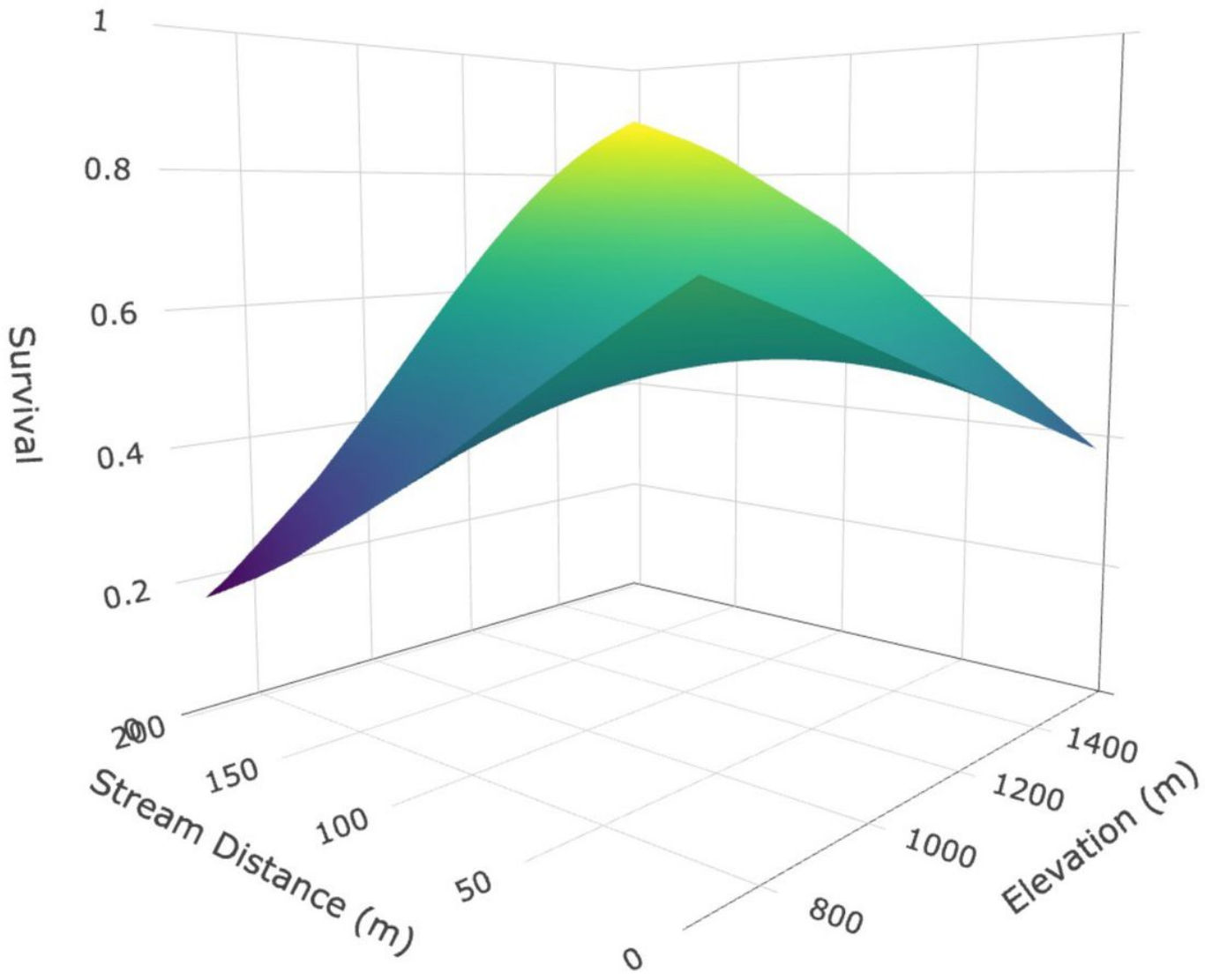

Figure 5

Interaction between elevation and stream distance on the survival probability of P. shermani estimated from the SEIPM. Survival probability is highest at low elevation and decreases with stream distance at lower elevations.

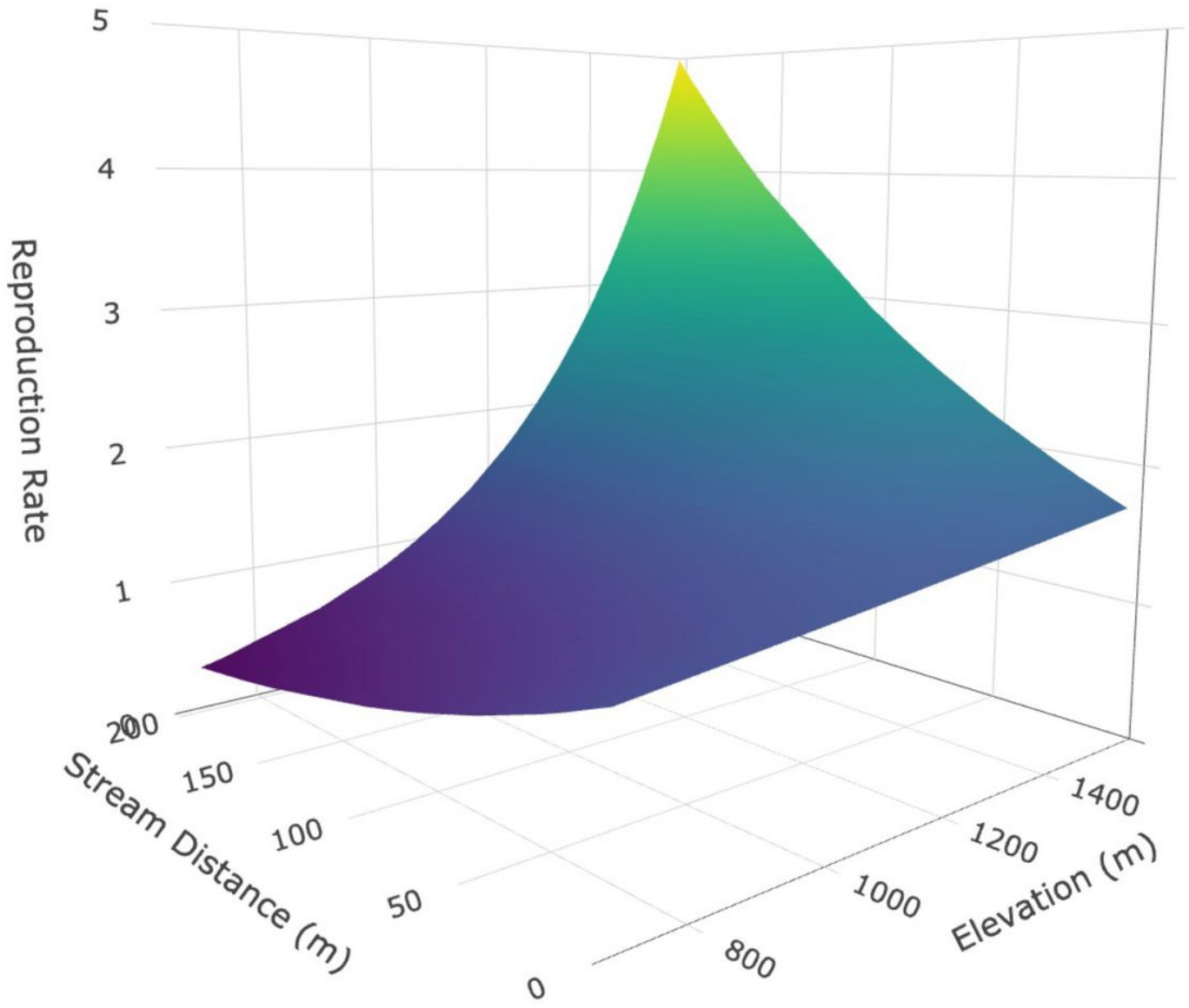

Figure 6

Interaction between elevation and stream distance on per capita reproduction rate of P. shermani estimated from the SEIPM. Per capita reproduction increases with elevation and at low elevations, decreases with stream distance.

Supplementary Files

This is a list of supplementary files associated with this preprint. Click to download.

- SuppInfo.docx